nature medicine

Heparanase promotes tumor infiltration and antitumor activity of CAR-redirected T lymphocytes

Ignazio Caruana[1], Barbara Savoldo[1,2], Valentina Hoyos[1], Gerrit Weber[1], Hao Liu[3], Eugene S Kim[4], Michael M Ittmann[5–7], Dario Marchetti[5] & Gianpietro Dotti[1,5,8]

Adoptive transfer of chimeric antigen receptor (CAR)-redirected T lymphocytes (CAR-T cells) has had less striking therapeutic effects in solid tumors[1–3] than in lymphoid malignancies[4,5]. Although active tumor-mediated immunosuppression may have a role in limiting the efficacy of CAR-T cells[6], functional changes in T lymphocytes after their *ex vivo* manipulation may also account for the reduced ability of cultured CAR-T cells to penetrate stroma-rich solid tumors compared with lymphoid tissues. We therefore studied the capacity of human *in vitro*–cultured CAR-T cells to degrade components of the extracellular matrix (ECM). In contrast to freshly isolated T lymphocytes, we found that *in vitro*–cultured T lymphocytes lack expression of the enzyme heparanase (HPSE), which degrades heparan sulfate proteoglycans, the main components of ECM. We found that *HPSE* mRNA is downregulated in *in vitro*–expanded T cells, which may be a consequence of *p53* (officially known as *TP53*, encoding tumor protein 53) binding to the *HPSE* gene promoter. We therefore engineered CAR-T cells to express HPSE and showed their improved capacity to degrade the ECM, which promoted tumor T cell infiltration and antitumor activity. The use of this strategy may enhance the activity of CAR-T cells in individuals with stroma-rich solid tumors.

CAR-T cells in *in vitro* cultures consist mostly of memory and effector lymphocytes characterized by potent cytotoxic function[1,4,7]. However, to exploit their effector functions *in vivo*, CAR-T cells must traffic to and accumulate in tumor sites. These processes involve a complex sequence of events, beginning with the adhesion of T cells to endothelial cells and followed by chemokine-chemokine receptor interactions, that modulates their extravasation into antigen-rich tissues[8–10]. During this process, T lymphocytes actively degrade the main components of the subendothelial basement membrane and the ECM, including the heparan sulfate proteoglycans (HSPGs)[11]. The ECM is an integral component of the stroma, and therefore T cells attacking stroma-rich solid tumors must be able to degrade HSPGs in order to access tumor cells and exert antitumor effects.

The release of specific enzymes by T cells is fundamental to the degradation of ECM. One of these enzymes is HPSE, which is the only known mammalian β-D-endoglycosidase capable of cleaving the heparan sulfate chains of HSPGs[9,12–14]. HPSE is first synthesized as a latent precursor protein of ~65 kDa and then cleaved into two subunits of ~8 and ~50 kDa that heterodimerize to form the enzymatically active protein[13]. HPSE is produced in large amounts by activated $CD4^+$ T lymphocytes, neutrophils, monocytes and B lymphocytes[15–17]. However, the exact contribution of HPSE in mediating the tumor infiltration of *in vitro*–cultured, tumor-specific T cells remains unexplored.

We first assessed whether *ex vivo*–expanded human T cells are defective in their capacity to degrade the ECM. Using a Matrigel-based cell invasion assay, we compared the invasion capacity of freshly isolated resting T cells (FI-T cells), briefly activated T cells (BA-T cells; 24 h of activation with CD3-specific (OKT3) and CD28-specific antibodies) and long-term *ex vivo*–expanded T cells (LTE-T cells; activation with OKT3 and CD28-specific antibodies and *ex vivo* culture for 12–14 d). Consistent with previously reported data in rodents[12], BA-T cells showed superior invasion of the ECM compared to FI-T cells (34% ± 8% vs. 23% ± 8%, respectively; $P = 0.05$). Conversely, LTE-T cells had a significantly reduced ability to degrade ECM (8% ± 6%) compared to both BA-T ($P = 0.01$) and FI-T ($P = 0.022$) cells (**Fig. 1a**). To dissect the mechanisms responsible for this observation, we evaluated the expression and function of HPSE in each cell population. In accordance with the cell invasion assay, both $CD4^+$ and $CD8^+$ T cells from FI-T and BA-T cells retained the active form of HPSE (50 kDa), whereas the enzyme was not detectable by western blotting and immunofluorescence in LTE-T cells (**Fig. 1b**,**c**). The loss of HPSE expression in LTE-T cells was not determined by the culture medium or cytokines used for T cell growth, as we observed similar results using either human type AB serum or fetal bovine serum, and interleukin (IL)-2, IL-7 or IL-15 as T cell growth factors (**Supplementary Fig. 1**). We also found that the loss of HPSE expression in response to stimulation with OKT3 and anti-CD28 antibodies and cytokines is observed in naive ($CD45RA^+$), central memory

[1]Center for Cell and Gene Therapy, Baylor College of Medicine and Houston Methodist Hospital, Houston, Texas, USA. [2]Department of Pediatrics, Texas Children's Hospital, Baylor College of Medicine, Houston, Texas, USA. [3]Biostatistics Shared Resource, Baylor College of Medicine, Houston, Texas, USA. [4]Department of Surgery, Texas Children's Hospital, Baylor College of Medicine, Houston, Texas, USA. [5]Department of Pathology and Immunology, Baylor College of Medicine, Houston, Texas, USA. [6]Interdepartmental Program in Translational Biology and Molecular Medicine, Baylor College of Medicine, Houston, Texas, USA. [7]Michael E. DeBakey Department of Veterans Affairs Medical Center, Dan L. Duncan Cancer Center, Houston, Texas, USA. [8]Department of Medicine, Baylor College of Medicine, Houston, Texas, USA. Correspondence should be addressed to G.D. (gdotti@bcm.edu).

Received 23 November 2014; accepted 27 February 2015; published online 13 April 2015; doi:10.1038/nm.3833

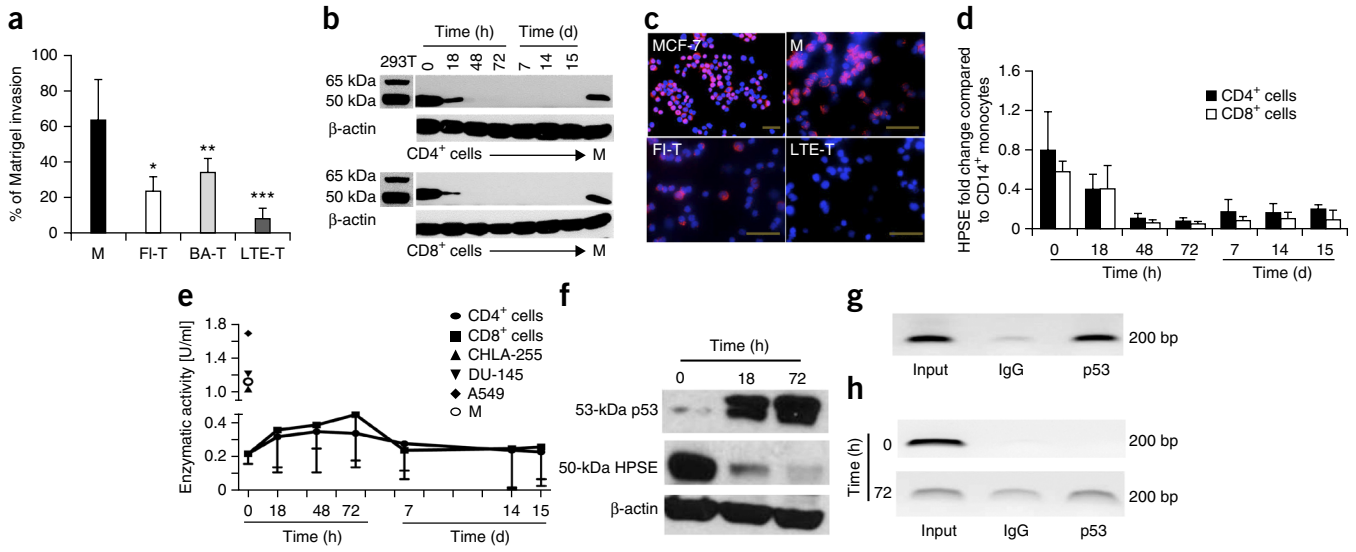

Figure 1 LTE-T cells show reduced invasion of the ECM and loss of the enzyme HPSE. (**a**) ECM invasion assay of CD14+ monocytes (M), FI-T cells, BA-T cells and LTE-T cells. Monocytes freshly isolated from peripheral blood showed the highest capacity to degrade the ECM (63% ± 23%). BA-T cells showed superior invasion of ECM compared to FI-T cells (**$P = 0.05$) and LTE-T cells (***$P = 0.01$), while LTE-T cells also showed inferior invasion compared to FI-T cells (*$P = 0.022$); analysis of variance (ANOVA) followed by a log-rank (Mantel–Cox) test for multiple comparisons. Data summarize means ± s.d. of five donors. We compared all four cell subsets for each donor. (**b**) Western blot showing the expression of HPSE in monocytes (M), CD4+ and CD8+ T cells at different culture time points. Data are representative of four donors. Positive controls are *HPSE*-transfected 293T cells. (**c**) Immunofluorescence staining for HPSE in MCF-7 cells, M, FI-T cells and LTE-T cells. Nuclei are stained with DAPI and shown in blue, whereas HPSE is stained with red fluorescent dye (Alexa Fluor 555). Magnification is 20×; scale bars, 50 µm. (**d**) qRT-PCR of *HPSE* in CD4+ and CD8+ T cells at different culture time points. Data summarize means ± s.d. of four donors. (**e**) HPSE enzymatic activity assessed in supernatants collected from CD4+ and CD8+ T cells at different culture time points. Monocytes and tumor cell lines CHLA-255, A549 and DU-145 are positive controls. Data summarize means ± s.d. of 4 donors. In **b**,**d**,**e** the condition 'day 15' indicates HPSE expression in LTE-T cells cultured for 14 d and re-stimulated with immobilized OKT3 and CD28-specific antibodies for 24 h to assess whether TCR re-stimulation can re-induce HPSE expression. (**f**) Western blot showing the expression of HPSE and full-length p53 protein in T cells before ($t = 0$) and after activation with immobilized OKT3 and CD28-specific antibodies for 18 and 72 h. Shown are results from one representative of three donors. (**g**,**h**) p53 ChIP in LTE-T cells cultured for 14 d (**g**), and in CD45RA+ cells before ($t = 0$) and after stimulation with OKT3 and CD28-specific monoclonal antibodies ($t = 72$ h) (**h**). Input is DNA that has been sonicated but not immunoprecipitated; IgG and p53 are DNA immunoprecipitated by the isotype and p53-specific antibody that recognizes the full-length protein. Relative quantification was performed comparing the intensities of PCR bands of IgG and p53 to input PCR band. For this representative sample, relative quantifications are: IgG, 20% and p53, 90% for LTE-T cells (**g**); IgG, 2% and p53, 4% at $t = 0$ and IgG, 53% and p53, 100% at $t = 72$ h for CD45RA+ cells (**h**). Shown is one representative of three donors.

(CD45RO+CD62L+) and effector memory (CD45RO+CD62L−) T cells isolated from the peripheral blood, suggesting that this is a general phenomenon and that it is not T cell subset specific (**Supplementary Fig. 2**). The absence of HPSE protein in LTE-T cells was associated with the downregulation of the *HPSE* mRNA. As shown in **Figure 1d**, *HPSE* mRNA decreased immediately after activation in both CD4+ and CD8+ T cells compared to CD14+ monocytes ($P < 0.005$ and $P < 0.031$, respectively) and remained low over the subsequent 14 d of culture. Re-stimulation of LTE-T cells with OKT3 and anti-CD28 antibodies on day 14 of culture did not induce re-expression of either the *HPSE* mRNA or protein (**Fig. 1b**,**d**). The lack of cellular HPSE in LTE-T cells was also confirmed by the absence of enzymatic activity in the culture supernatant. As shown in **Figure 1e**, HPSE enzymatic activity was detected in supernatants collected within the first 72 h after activation of FI-T cells. This detection can be attributed to enzyme accumulation in the culture medium. However, the enzymatic activity returned to background levels 72 h later (from 0.34 ± 0.2 U ml and 0.45 ± 0.27 U ml to 0.22 ± 0.06 U ml) for both CD4+ and CD8+ T cells (**Fig. 1e**). This observation is in line with previous studies reporting that preformed HPSE protein is stored in an intracellular compartment and released as an early event in response to T cell activation[18]. We found that HPSE is also absent in Epstein–Barr virus–specific cytotoxic T cells that are stimulated *in vitro* by antigen-presenting cells, suggesting that HPSE loss in LTE-T cells is not caused by a supra-physiological activation of these cells mediated by OKT3 antibody[19] (**Supplementary Fig. 2**). Previous studies showed that mutated *p53* with loss of function in tumor cells is associated with overexpression of HPSE[20]. Because there is an accumulation of full-length p53 in LTE-T cells[20,21], we suggest that the lack of *HPSE* mRNA expression in LTE-T cells may be due to the accumulation of full-length p53 in LTE-T cells, which binds to the *HPSE* gene promoter (**Fig. 1f–h** and **Supplementary Fig. 3**). The immediate translational implication of these findings is that T cells that are engineered *in vitro* and cultured for adoptive immunotherapy lack HPSE expression when infused into subjects, and they are thus impaired in their capacity to degrade components of the ECM of the stroma. It is also important to note that the cleavage of HPSG chains by HPSE releases preformed stored chemokines into the stroma[22,23]. Because chemokines also guide the migration of T cells toward their target cells within the tumor microenvironment, the lack of HPSE may further indirectly compromise the antitumor effects of T cells by reducing their migration.

We thus hypothesized that engineering LTE-T cells to express HPSE through retroviral gene transfer would improve their invasion capability. LTE-T cells transduced with the HPSE(I)GFP retroviral vector expressed GFP (**Fig. 2a**) and HPSE (**Fig. 2b**). HPSE expression

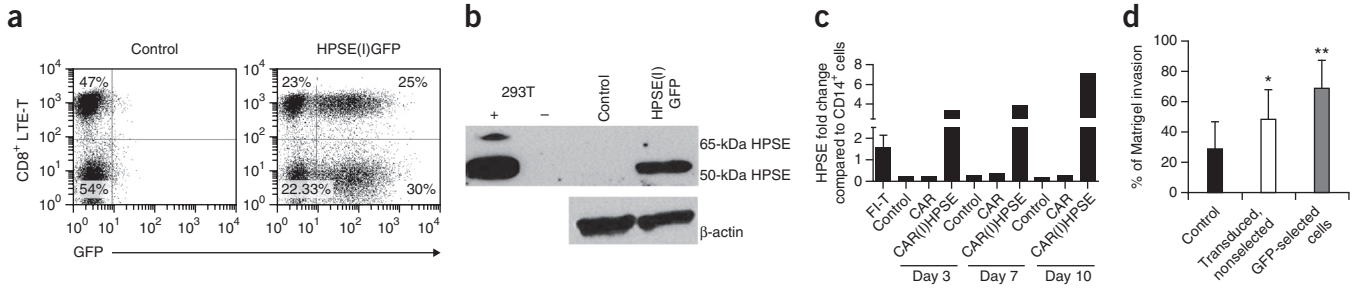

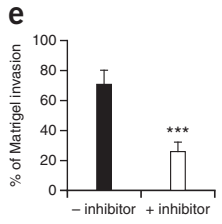

Figure 2 LTE-T cells modified to express HPSE show enhanced degradation of the ECM. We transduced LTE-T cells with retroviral vectors encoding *HPSE* and GFP (HPSE(I)GFP) or both the GD2-specific CAR and *HPSE* (CAR(I)HPSE). (**a**) GFP expression by both CD4$^+$ and CD8$^+$ LTE-T cells at days 12–14 of culture. (**b**) Western blot showing the expression of HPSE in control and transduced LTE-T cells at days 12–14 of culture. (**c**) qRT-PCR of *HPSE* in control and CAR(I)HPSE$^+$ LTE-T cells cultured in IL-2 deficient medium for 3, 7 and 10 d. Data are representative of two donors. (**d**) HPSE(I)GFP$^+$ LTE-T cells were sorted based on GFP expression. After sorting we used the ECM invasion assay to compare control, nonsorted HPSE(I)GFP$^+$ LTE-T cells and GFP-sorted HPSE(I)GFP$^+$ LTE-T cells. Data summarize mean ± s.d. of nine donors, $^*P = 0.025$; $^{**}P < 0.001$. (**e**) ECM invasion assay of *HPSE*-transduced LTE-T cells in the presence or absence of the inhibitor heparin H1. Data summarize mean ± s.d. of four donors, $^{***}P < 0.01$; Student's *t*-test.

remained high in transduced LTE-T cells starved of cytokines in culture for more than 10 d, suggesting stable transgene expression (**Fig. 2c**). In functional assays, HPSE(I)GFP$^+$ LTE-T cells better degraded ECM (48% ± 19%) than did control untransduced LTE-T cells (29% ± 18%; $P = 0.025$) (**Fig. 2d**). The addition of the HPSE inhibitor heparin H1 (ref. 24) confirmed that the invasion of HPSE(I)GFP$^+$

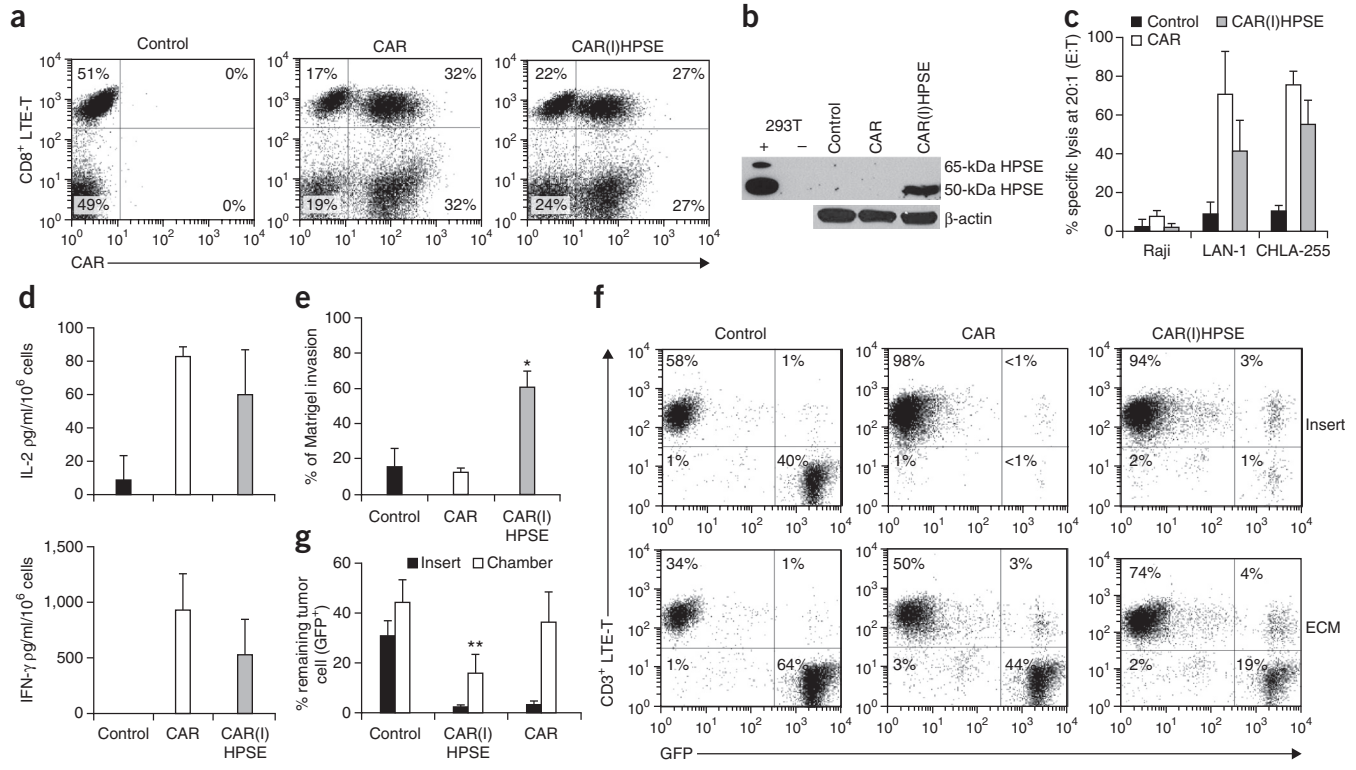

Figure 3 LTE-T cells co-expressing *HPSE* and GD2-specific CAR retain GD2 specificity and have enhanced capacity to degrade ECM. We transduced LTE-T cells with retroviral vectors encoding either the GD2-specific CAR alone (CAR) or both the GD2-specific CAR and *HPSE* (CAR(I)HPSE). (**a**) Flow cytometry analysis to detect CAR expression by control and transduced LTE-T cells. (**b**) Western blot to detect HPSE in control and transduced LTE-T cells. Data are representative of five donors. (**c**) Cytotoxic activity of control, CAR$^+$ and CAR(I)HPSE$^+$ LTE-T cells assessed by ^{51}Cr-release assay at a 20:1 E:T ratio. We used LAN-1 and CHLA-255 cells (GD2$^+$), and Raji cells (GD2$^-$) as target cells. (**d**) Transduced LTE-T cells release both IL-2 and IFN-γ in response to GD2$^+$ tumor cells. (**e**) Invasion of ECM by control, CAR$^+$ and CAR(I)HPSE$^+$ LTE-T cells. Data in **c**–**e** summarize mean ± s.d. from five donors, $^*P = 0.004$; Student's *t*-test. (**f**,**g**) We plated control and transduced LTE-T cells in the upper chamber of the Matrigel invasion assay either with ECM or without ECM (insert), and LAN-1-GFP$^+$ cells in the lower chamber. After day 3 of culture, we collected cells in the lower chamber to quantify CD3$^+$ T cells and GFP$^+$ tumor cells by flow cytometry. (**f**) illustrates representative dot plots of the flow cytometry of CD3$^+$ T cells versus GFP$^+$ tumor cells, whereas (**g**) summarizes mean ± s.d. of residual GFP$^+$ tumor cells of five donors, $^{**}P = 0.009$. In all cases we analyzed LTE-T cells by days 12–14 of culture.

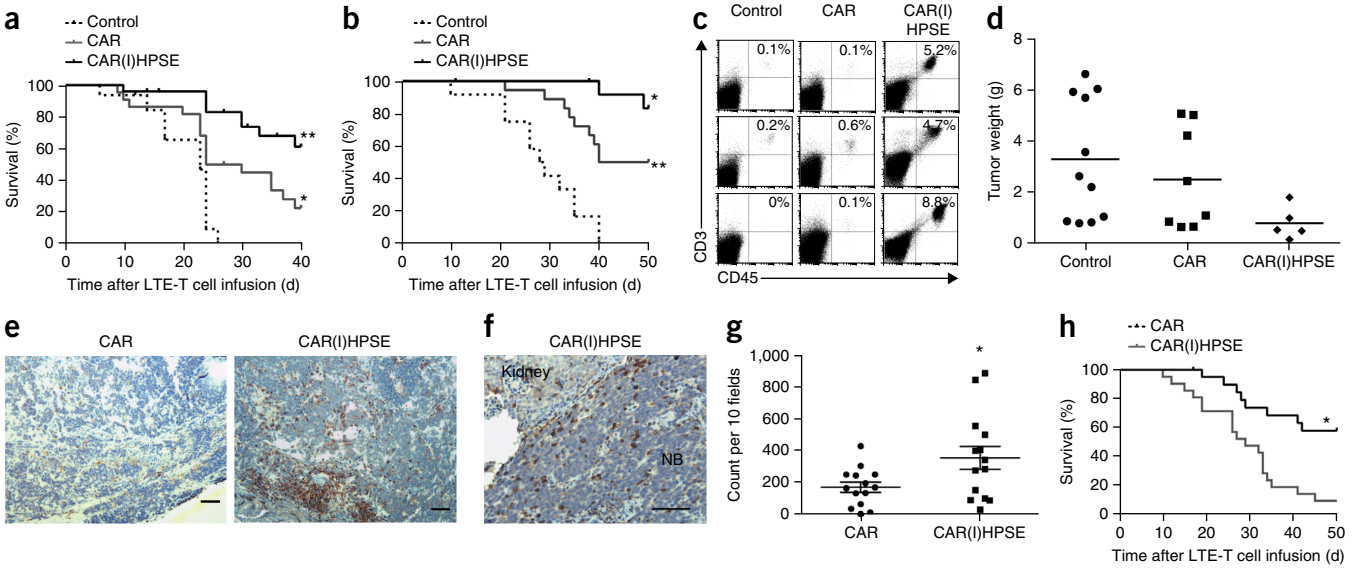

Figure 4 CAR-GD2$^+$ LTE-T cells co-expressing *HPSE* show enhanced tumor infiltration and improve overall survival in xenograft tumor models. (**a**) Kaplan–Meier analysis of mice engrafted i.p. with the tumor cell line CHLA-255 and treated i.p. with control, CAR$^+$ and CAR(I)HPSE$^+$ LTE-T cells. Shown are data from three independent experiments using LTE-T cells generated from three donors. Control, $n = 16$; CAR, $n = 22$; CAR(I)HPSE, $n = 26$ mice; $^*P < 0.007$, $^{**}P < 0.0001$. (**b**) Kaplan–Meier analysis of mice engrafted i.p. with the tumor cell line LAN-1 and treated i.p. with control, CAR$^+$ and CAR(I)HPSE$^+$ LTE-T cells. For these experiments, we generated LTE-T cells from two donors. Control, $n = 12$; CAR, $n = 18$; CAR(I)HPSE, $n = 14$ mice; $^*P = 0.039$, $^{**}P < 0.0001$. (**c**) Flow cytometry analysis of CD3$^+$ T cells detected within the tumor samples. Dot plots are representative of three mice per group from mice infused with LTE-T cells generated from the same donor. (**d**) Weight of the tumors collected from euthanized mice engrafted with LAN-1 tumor cells. (**e**,**f**) Immunohistochemical analysis showing CD3$^+$ T cell infiltration in NB tumor CHLA-255 cells implanted in the kidney of mice infused with either CAR$^+$ or CAR(I)HPSE$^+$ LTE-T cells. 100× magnification (**e**) and 200× magnification (**f**); scale bars, 100 µm. (**g**) The graph shows the numbers of infiltrating CD3$^+$ T cells per ten high-power fields in tumors collected from mice treated with either CAR$^+$ or CAR(I)HPSE$^+$ LTE-T cells (cell numbers 357 ± 72 and 173 ± 32, respectively), $^*P = 0.028$. (**h**) Kaplan-Meier analysis of mice surgically implanted under the renal capsule with CHLA-255 NB cells and infused i.v. with either CAR$^+$ or CAR(I)HPSE$^+$ LTE-T cells. For these experiments, we generated LTE-T cells from two donors, CAR, $n = 21$; CAR(I)HPSE, $n = 21$ mice; $^*P = 0.0006$.

LTE-T cells is HPSE-specific, as invasion was reduced from 74% ± 14% in the absence of inhibitor to 29% ± 9% ($P < 0.01$) in the presence of heparin H1 (**Fig. 2e**). We then assessed whether HPSE expression leading to improved cell invasion could be coupled with antitumor specificity. We used neuroblastoma (NB) as a cancer model because this tumor type has been targeted in a clinical trial with a CAR specific to the NB-associated antigen GD2 with some clinical responses[1]. On day 14 of culture, CAR expression was 71% ± 14% and 56% ± 6% in LTE-T cells transduced with CAR and CAR(I)HPSE vectors, respectively (**Fig. 3a**). HPSE was detected only in LTE-T cells transduced with the CAR(I)HPSE vector (**Fig. 3b**). Both CAR$^+$ and CAR(I)HPSE$^+$ LTE-T cells lysed the GD2$^+$ human NB cell line LAN-1 (71% ± 22% and 41% ± 16%, respectively, at a 20:1 effector-to-target cell (E:T) ratio in a ^{51}Cr-release assay)(P = nonsignificant (ns)), and the GD2$^+$ human NB cell line CHLA-255 (76% ± 7% and 55% ± 13%, respectively) (P = ns), whereas both CAR$^+$ and CAR(I)HPSE$^+$ LTE-T cells showed negligible activity against the GD2$^-$ Raji cell line (<8%) (**Fig. 3c**). Control LTE-T cells lacking the CAR lysed none of these targets. The cytolytic activity was associated with a preserved T_H1 cytokine profile, as CAR$^+$ and CAR(I)HPSE$^+$ LTE-T released similar amounts of interferon (IFN)-γ (927 ± 328 and 527 ± 320 pg/ml × 10^6 cells, respectively; P = ns) and IL-2 (83 ± 6 and 61 ± 27 pg/ml × 10^6 cells, respectively, P = ns) in response to stimulation with GD2$^+$ tumor cells (**Fig. 3d**). In sharp contrast to their comparable cytolytic function, only CAR(I)HPSE$^+$ LTE-T cells degraded the ECM (66% ± 1%) compared to CAR$^+$ or control LTE-T cells (13% ± 9% and 16% ± 10%, respectively) ($P = 0.004$ and $P < 0.001$) (**Fig. 3e**). To prove *ex vivo* that LTE-T cells co-expressing *HPSE* and CAR have increased antitumor activity in the presence of ECM, we plated LTE-T and tumor cells in a Matrigel cell invasion assay, in which LTE-T cells must degrade the ECM to reach and eliminate the tumor targets. After 3 d of culture, both CAR$^+$ and CAR(I)HPSE$^+$ LTE-T cells eliminated LAN-1 tumor cells equally well in the absence of the ECM (<3% GFP$^+$ tumor cells) compared to control LTE-T cells (31% ± 6% GFP$^+$ tumor cells) (**Fig. 3f**,**g**). By contrast, in the presence of ECM, CAR(I)HPSE$^+$ LTE-T cells eliminated all but 16% ± 8% of LAN-1 cells, compared to 37% ± 12% in the presence of CAR$^+$ LTE-T cells ($P = 0.001$) (**Fig. 3f**,**g**). Control LTE-T cells did not show antitumor activity (45% ± 9% GFP$^+$ tumor cells). We obtained identical results with the CHLA-255 human NB cell line (**Supplementary Fig. 4**). Thus, only LTE-T cells co-expressing *HPSE* and CAR show robust antitumor activity in the presence of the ECM. The improved antitumor activity of CAR(I)HPSE$^+$ LTE-T cells was achieved without causing detectable detrimental effects on T lymphocytes. Indeed, CAR(I)HPSE$^+$ LTE-T cells expanded *in vitro*, retained the same phenotype of CAR$^+$ LTE-T cells and did not show increased activation-induced cell death in response to either OKT3-specific antibody, which binds CD3, or 1A7 anti-idiotype antibody, which causes cross-linking of the GD2-specific CAR[1] (**Supplementary Fig. 5**).

To validate our findings *in vivo*, we first established xenograft models of NB by implanting NSG-strain mice intraperitoneally (i.p.) with either CHLA-255 or LAN-1 NB cell lines in the presence of Matrigel to allow the formation of complex and structured tumors. We used the i.p. route to minimize confounding variables related to T cell homing to the tumor, a known issue in NB xenograft models when the tumor is inoculated subcutaneously[25]. After 10 d, mice received

either control, CAR+ or CAR(I)HPSE+ LTE-T cells i.p. As shown in **Figure 4a**, mice implanted with CHLA-255 tumor cells and treated with CAR(I)HPSE+ LTE-T cells had significantly improved survival by day 40 compared to mice treated with control LTE-T ($P < 0.001$) or CAR+ LTE-T ($P < 0.007$) cells. Among treated mice, we found that 6 of 22 infused with CAR+ LTE-T cells, and 18 of 26 infused with CAR(I)HPSE+ LTE-T cells were macroscopically tumor free when we ended the observation at day 40 ($P = 0.008$). We obtained similar results in mice engrafted with LAN-1 tumor cells. Mice infused with CAR(I)HPSE+ LTE-T cells had significantly improved survival compared to mice treated with control ($P < 0.0001$) or CAR+ LTE-T cells at day 50 ($P < 0.039$) (**Fig. 4b** and **Supplementary Fig. 6**). In another set of experiments, we euthanized mice on day 12–14 after T cell infusion to measure tumor T cell infiltration. Tumors collected from mice infused with CAR(I)HPSE+ LTE-T cells had greater T cell infiltration (4.6% ± 2.4%) compared to those treated with control (0.6% ± 0.5; $P = 0.029$) or CAR+ LTE-T cells (0.1% ± 0.1; $P = 0.043$) (**Fig. 4c**). Tumors collected from euthanized mice also showed a significant reduction in weight in recipients infused with CAR(I)HPSE+ LTE-T cells compared to control (0.8 g ± 0.6 g vs. 3.3 g ± 2.4 g) ($P = 0.039$), and when compared to mice infused with CAR+ LTE-T cells (0.8 g ± 0.6 g vs. 2.5 g ± 2 g), although this difference was not statistically significant ($P = 0.093$) (**Fig. 4d**). Because NB cell lines require Matrigel to form complex and structured tumors when infused i.p., we also implemented a third NB model in which CHLA-255 tumor cells labeled with firefly luciferase were implanted in the kidney of Nod scid gamma (NSG) mice without using Matrigel[26], and CAR+ LTE-T and CAR(I)HPSE+ LTE cells were infused intravenously (i.v.). Tumor sections from mice infused i.v. with CAR(I)HPSE+ LTE-T cells showed enhanced infiltration of CD3+ T cells compared to CAR+ LTE-T cells (357 ± 72 and 173 ± 32 cells, respectively; $P = 0.028$) (**Fig. 4e–g**). Long-term observation of infused mice also showed improved survival of recipients treated with CAR(I)HPSE+ LTE-T cells by day 50 ($P < 0.005$) (**Fig. 4h** and **Supplementary Fig. 6**).

Finally, we extended our observation to CAR+ LTE-T cells targeting the solid tumor-associated antigen chondroitin sulfate proteoglycan 4 (CSPG4)[27] in an aggressive melanoma model, suggesting that the positive effect of HPSE in CAR-T cells can be extrapolated to other targeted antigens and solid tumors (**Supplementary Fig. 7**). In contrast, the co-expression of HPSE in LTE-T cells redirected with a CD19-specific CAR did not seem to have a role in B-lymphoid malignancies, which are generally stroma-poor compared to solid tumors (**Supplementary Fig. 8**).

Under physiological conditions, HPSE expression by T cells is regulated to avoid tissue damage from T cell extravasation into nonpathologic tissues[16,17,28,29]. To rule out concerns about non-specific infiltration of normal tissues, such as lung or liver, by *HPSE*-engineered LTE-T cells, we evaluated *in vivo* T cell biodistribution. For these experiments, we labeled CAR(I)HPSE+ and CAR+ LTE-T cells with the vector encoding GFP and firefly luciferase and infused them via tail injection. T cell biodistribution evaluated by *in vivo* imaging at different time points after T cell inoculation and immunohistochemical analysis at early and late passages did not show differences between the two groups of mice, suggesting no preferential accumulation in lung or liver of *HPSE*-engineered LTE-T cells (**Supplementary Fig. 9a**,**b**).

In conclusion, HPSE deficiency in *in vitro*–engineered and cultured tumor-specific LTE-T cells may limit their antitumor activity in stroma-rich solid tumors. Other enzymes such as matrix metalloproteases (MMPs) are also involved in modifications of ECM components and may compensate for HPSE deficiency[30]. However, we found that some MMPs are also downregulated upon TCR activation and cytokine exposure (**Supplementary Fig. 10a**,**b**). We thus suggest that inducing expression of HPSE in LET-T cells co-expressing a tumor-specific CAR improves their capacity to degrade the ECM without compromising their viability, expansion or effector function, and it promotes increased antitumor activity. The proposed strategy may enhance the antitumor activity of CAR-redirected T cells in subjects with stroma-rich solid tumors.

METHODS

Methods and any associated references are available in the online version of the paper.

Note: Any Supplementary Information and Source Data files are available in the online version of the paper.

ACKNOWLEDGMENTS

The authors would like to thank I.Vlodavsky and M. Brenner for the critical review of the manuscript and C. Gillespie for editing. This work was supported in part by the US National Institutes of Health-National Cancer Institute (G.D., no. R01 CA142636) and by a Department of Defense and Technology and Therapeutic Development Award (G.D., no. W81XWH-10-10425). L. Metelitsa kindly provided the CHLA-255 human NB cell line.

AUTHOR CONTRIBUTIONS

G.D., I.C. and B.S. designed experiments; I.C., V.H., G.W. and E.S.K. performed the experiments; I.C., B.S. and G.D. analyzed the data; I.C. and G.D. wrote the manuscript; H.L. performed the statistical analysis; M.M.I. performed the pathology; D.M. provided his expertise in the heparanase field and provided crucial reagents; all the authors reviewed and approved the final version of the manuscript.

COMPETING FINANCIAL INTERESTS

The authors declare competing financial interests: details are available in the online version of the paper.

1. Pule, M.A. *et al.* Virus-specific T cells engineered to coexpress tumor-specific receptors: persistence and antitumor activity in individuals with neuroblastoma. *Nat. Med.* **14**, 1264–1270 (2008).
2. Kershaw, M.H. *et al.* A phase I study on adoptive immunotherapy using gene-modified T cells for ovarian cancer. *Clin. Cancer Res.* **12**, 6106–6115 (2006).
3. Bawley, V.S. *et al.* T cells redirected against HER2 for adoptive immunotherapy for HER2-positive osteosarcoma. *Cancer Res.* **72**, 3500 (2012).
4. Kalos, M. *et al.* T cells with chimeric antigen receptors have potent antitumor effects and can establish memory in patients with advanced leukemia. *Sci. Transl. Med.* **3**, 95ra73 (2011).
5. Brentjens, R.J. *et al.* CD19-targeted T cells rapidly induce molecular remissions in adults with chemotherapy-refractory acute lymphoblastic leukemia. *Sci. Transl. Med.* **5**, 177ra38 (2013).
6. Zou, W. Immunosuppressive networks in the tumour environment and their therapeutic relevance. *Nat. Rev. Cancer* **5**, 263–274 (2005).
7. Savoldo, B. *et al.* CD28 costimulation improves expansion and persistence of chimeric antigen receptor-modified T cells in lymphoma patients. *J. Clin. Invest.* **121**, 1822–1826 (2011).
8. Muller, W.A. Leukocyte-endothelial-cell interactions in leukocyte transmigration and the inflammatory response. *Trends Immunol.* **24**, 327–334 (2003).
9. Parish, C.R. The role of heparan sulphate in inflammation. *Nat. Rev. Immunol.* **6**, 633–643 (2006).
10. Yadav, R., Larbi, K.Y., Young, R.E. & Nourshargh, S. Migration of leukocytes through the vessel wall and beyond. *Thromb. Haemost.* **90**, 598–606 (2003).
11. Bernfield, M. *et al.* Functions of cell surface heparan sulfate proteoglycans. *Annu. Rev. Biochem.* **68**, 729–777 (1999).
12. de Mestre, A.M., Staykova, M.A., Hornby, J.R., Willenborg, D.O. & Hulett, M.D. Expression of the heparan sulfate-degrading enzyme heparanase is induced in infiltrating CD4+ T cells in experimental autoimmune encephalomyelitis and regulated at the level of transcription by early growth response gene 1. *J. Leukoc. Biol.* **82**, 1289–1300 (2007).
13. Vlodavsky, I., Ilan, N., Naggi, A. & Casu, B. Heparanase: structure, biological functions, and inhibition by heparin-derived mimetics of heparan sulfate. *Curr. Pharm. Des.* **13**, 2057–2073 (2007).

14. Yurchenco, P.D. & Schittny, J.C. Molecular architecture of basement membranes. *FASEB J.* **4**, 1577–1590 (1990).
15. Fridman, R. *et al.* Soluble antigen induces T lymphocytes to secrete an endoglycosidase that degrades the heparan sulfate moiety of subendothelial extracellular matrix. *J. Cell. Physiol.* **130**, 85–92 (1987).
16. Naparstek, Y., Cohen, I.R., Fuks, Z. & Vlodavsky, I. Activated T lymphocytes produce a matrix-degrading heparan sulphate endoglycosidase. *Nature* **310**, 241–244 (1984).
17. Vlodavsky, I. *et al.* Expression of heparanase by platelets and circulating cells of the immune system: possible involvement in diapedesis and extravasation. *Invasion Metastasis* **12**, 112–127 (1992).
18. Bartlett, M.R., Underwood, P.A. & Parish, C.R. Comparative analysis of the ability of leucocytes, endothelial cells and platelets to degrade the subendothelial basement membrane: evidence for cytokine dependence and detection of a novel sulfatase. *Immunol. Cell Biol.* **73**, 113–124 (1995).
19. Smith, C.A. *et al.* Production of genetically modified Epstein-Barr virus-specific cytotoxic T cells for adoptive transfer to patients at high risk of EBV-associated lymphoproliferative disease. *J. Hematother.* **4**, 73–79 (1995).
20. Baraz, L., Haupt, Y., Elkin, M., Peretz, T. & Vlodavsky, I. Tumor suppressor p53 regulates heparanase gene expression. *Oncogene* **25**, 3939–3947 (2006).
21. Mondal, A.M. *et al.* p53 isoforms regulate aging- and tumor-associated replicative senescence in T lymphocytes. *J. Clin. Invest.* **123**, 5247–5257 (2013).
22. Gallagher, J.T. Heparan sulfate: growth control with a restricted sequence menu. *J. Clin. Invest.* **108**, 357–361 (2001).
23. Iozzo, R.V. Matrix proteoglycans: from molecular design to cellular function. *Annu. Rev. Biochem.* **67**, 609–652 (1998).
24. Nakajima, M., Irimura, T., Di, F.N. & Nicolson, G.L. Metastatic melanoma cell heparanase. Characterization of heparan sulfate degradation fragments produced by B16 melanoma endoglucuronidase. *J. Biol. Chem.* **259**, 2283–2290 (1984).
25. Craddock, J.A. *et al.* Enhanced tumor trafficking of GD2 chimeric antigen receptor T cells by expression of the chemokine receptor CCR2b. *J. Immunother.* **33**, 780–788 (2010).
26. Patterson, D.M., Shohet, J.M. & Kim, E.S. Preclinical models of pediatric solid tumors (neuroblastoma) and their use in drug discovery. *Curr. Protoc. Pharmacol.* **52**, 14.17.1–14.17.18 (2011).
27. Geldres, C. *et al.* T lymphocytes redirected against the chondroitin sulfate proteoglycan-4 control the growth of multiple solid tumors both *in vitro* and *in vivo*. *Clin. Cancer Res.* **20**, 962–971 (2014).
28. Arvatz, G., Barash, U., Nativ, O., Ilan, N. & Vlodavsky, I. Post-transcriptional regulation of heparanase gene expression by a 3′ AU-rich element. *FASEB J.* **24**, 4969–4976 (2010).
29. Lu, W.C., Liu, Y.N., Kang, B.B. & Chen, J.H. Trans-activation of heparanase promoter by ETS transcription factors. *Oncogene* **22**, 919–923 (2003).
30. Wilson, T.J. & Singh, R.K. Proteases as modulators of tumor-stromal interaction: primary tumors to bone metastases. *Biochim. Biophys. Acta* **1785**, 85–95 (2008).

ONLINE METHODS

Cell lines. 293T, DU-145 and CHLA-255 cell lines were cultured in IMDM (Gibco, Invitrogen, Carlsbad, CA) supplemented with 10% FBS (FBS, HyClone, Thermo Scientific, Pittsburgh, PA) and 2 mM GlutaMax (Invitrogen, Carlsbad, CA). MCF-7, Raji, K562, LAN-1, Daudi and SENMA cells were cultured in RPMI1640 (HyClone) supplemented with 10% FBS and 2 mM GlutaMax. A549 cells were cultured in DMEM (GIBCO) supplemented with 10% FBS and 2 mM GlutaMax. Cells were maintained in a humidified atmosphere containing 5% CO_2 at 37 °C. Tumor cell lines MCF-7, CHLA-255, A549 and DU-145 produced HPSE. All cell lines were routinely tested for mycoplasma and for surface expression of target antigens. Furthermore, all cell lines were authenticated except for CHLA-255, which was established from a neuroblastoma subject and SENMA, which was established in our laboratory from a melanoma subject[31]. However, we routinely verified that this line retained the surface expression of the target antigens.

Isolation and culture of primary human T lymphocytes. Peripheral blood mononuclear cells (PBMCs) were isolated from samples obtained from healthy volunteers from the protocol entitled 'Humoral and cellular immune responses to tumor-associated antigens (TAA)—healthy blood and skin donors' which is being conducted after approval by the Institutional Review Board of Baylor College of Medicine, or anonymous buffy coats (purchased as discarded material from the blood bank) of healthy donors (Gulf Coast Regional Blood Center, Houston, TX) using Lymphoprep density separation (Fresenius Kabi Norge, Oslo, Norway). Monocytes were obtained from PBMCs by positive magnetic selection with CD14 microbeads (Miltenyi Biotec, Auburn, CA). $CD8^+$ and $CD4^+$ T cells were also obtained from PBMCs by negative magnetic selection (Miltenyi Biotec). In selected experiments, naive ($CD45RA^+$), central-memory ($CD45RO^+CD62L^+$) and effector-memory ($CD45RO^+CD62L^-$) T cells were also separated from PBMC by CD45RA depletion and CD62L positive paramagnetic selection (Miltenyi Biotec). T lymphocytes were activated with immobilized OKT3 (1 μg/ml) and anti-CD28 (no. 555725, Becton Dickinson Biosciences, Franklin Lakes, NJ) (1 μg/ml) antibodies and then expanded in complete medium containing 45% RPMI 1640 and 45% Click's medium (Irvine Scientific, Santa Ana, CA, USA) supplemented with 10% FBS and 2 mM GlutaMax. Cells were fed twice a week with recombinant interleukin-2 (IL-2) (50 U mL) (Chiron Therapeutics, Emeryville, CA). We defined as FI-T cells: freshly isolated resting T cells from peripheral blood that comprise naive, effector-memory and central-memory T cells; BA-T cells: briefly activated T cells that result from incubation of FI-T with OKT3 and CD28-specific antibodies for 24 h; LTE-T cells: long-term *ex vivo* expanded T cells that result from BA-T cultured *ex vivo* for 12–14 d and consist mostly of central-memory and effector-memory T cells. At day 14 of culture, LTE-T cells were reactivated with OKT3 and CD28-specific antibodies and cultured for additional 24 h. For the experiments in which we compared the invasion capacity of FI-T versus BA-T versus LTE-T cells side by side, we obtained three separated blood draws at different time points from the donors to make LTE-T, BA-T and FI-T cells to be able to run all the samples in parallel in the invasion assay.

Cell invasion assay. The capacity of each cell subset to degrade ECM was examined *in vitro* using the BioCoat Matrigel Invasion assay (Becton Dickinson Biosciences) according to the manufacturer's instructions. Five percent FBS was used as a chemoattactant in the low chamber. All experiments were performed in duplicate. Data are expressed as the percentage of invasion through the Matrigel and the membrane relative to the migration through the control membrane (8 μm polyethylene terephthalate membrane pores). The percentage of invasion was calculated as follows: (mean of cells invading through the Matrigel chamber membrane/mean of cells migrating through the control insert membrane) × 100. In specific experiments, we simultaneously evaluated the invasion and antitumor activity of LTE-T cells. Briefly, we used the BioCoat Matrigel Invasion assay and plated LAN-1-GFP^+ or CHLA-255-GFP^+ cells (1.4×10^5) in the bottom of a 24-well plate and LTE-T cells (2.5×10^5 cells) in the upper chamber/insert. Chambers and inserts were removed 24 h later. After 3 d of culture cells were then collected from the lower chamber and quantified by flow cytometry to identify tumor cells and T cells, respectively.

Western blotting. 20 μg of proteins were resolved by SDS-PAGE and transferred to polyvinylidene difluoride membranes (Bio-Rad, Hercules, CA). The antibodies and dilutions used in these experiments were as follows: mouse anti-human HPA1-HPSE (1:100 and 1:6500 dilution, clone nos. HP130 and HP3-17, respectively) (InSight Biopharmaceuticals Ltd., Rehovot, Israel) that recognizes both the 65-kDa precursor and the 50-kDa active form of HPSE-1, rabbit anti-human HPA1 polyclonal (1:4000 dilution) (no. CLANT155, Cedarlane, Burlington, NC), mouse anti-human *p53* (1:200 dilution, clone DO-1) (Santa Cruz Biotechnology, Santa Cruz, CA) that recognizes the full-length *p53* protein, mouse anti-human β-actin (1:10000 dilution, clone C4) (Santa Cruz Biotechnology) and horseradish peroxidase–conjugated secondary antibodies (1:5,000 dilution, goat anti-mouse no. sc-2005 and goat anti-rabbit no. sc-2004) (Santa Cruz Biotechnology). Blots were then incubated with SuperSignal West Femto Maximum Sensitivity Substrate (Thermo Scientific).

Immunofluorescence. Cells were fixed with 4% paraformaldehyde. After permeabilization with 0.1% Triton X-100, cells were incubated with 5% goat serum (Cell Signaling Technology, Danvers, MA) and 1% BSA to block nonspecific binding. Cells were then stained with the primary antibody against human HPSE1 (HPA1, clone HP130) (InSight Biopharmaceuticals Ltd.) (1:100 dilution at 25 °C for 2 h). Cells were then probed with Alexa Fluor 555 goat anti-mouse secondary antibody (no. 44095, 1:500 dilution at 25 °C for 2 h) (Cell Signaling Technology). Fluorescent signals were detected using a fluorescence microscope (Olympus IX70, Leeds Instruments Inc., Irving, TX). DAPI (BioLegend, San Diego, CA) was used for nuclear staining.

RNA isolation and quantitative real-time PCR (qRT-PCR). For the qRT-PCR, 100 ng of total RNA was used to prepare cDNA (TaqMan One Step PCR Master Mix Reagents Kit) (Applied Biosystems, Carlsbad, CA). Specific primers and probes that were designed, tested, and standardized by Applied Biosystems for *HPSE* and *p53* were used (*HPSE*: Hs00935036_m1; *p53*: Hs01034249_m1). The difference in cycle threshold values (ΔCT) of *HPSE* was normalized to the ΔCT of *GAPDH* (glyceraldehyde-3-phosphate dehydrogenase, Hs99999905_m1), and the fold change in expression was expressed relative to $CD14^+$ monocytes, considered as a positive control while mesemchymal stem cells were used as a negative control. For *p53* mRNA quantification the difference in cycle threshold values (ΔCt) of *p53* was normalized to the ΔCt of *GAPDH* (glyceraldehyde-3-phosphate dehydrogenase, Hs99999905_m1), and the fold change in expression was expressed relative to FI-T cells.

Enzyme-linked immunosorbent assay (ELISA). Cytokine release by LTE-T cells in response to stimulation with $GD2^+$ LAN-1 cells was analyzed using IFN-γ and IL-2–specific ELISAs (R&D Systems, Minneapolis, MN). HPSE activity was measured using a heparan sulfate (HS) degrading enzyme assay kit (Takara Bio Inc., Otsu, Shiga, Japan). HPSE activity was measured in supernatants collected at different time point of culture of T lymphocytes. At days 4 and 14 of culture, T cells were collected, washed and re-suspended in fresh medium. As basal level of HPSE release we used nonactivated T cells rested for 48–72 h in medium. Supernatant from $CD14^+$ monocytes and tumor cell lines were used as positive control. HPSE activity was determined as the inverse of decrease in absorbance as previously described[32,33]. T cell and tumor cell supernatants were analyzed in triplicate.

Multiplex for matrix metalloproteases (MMPs). Analysis of MMPs was performed using Milliplex Map kit panel 1 and 2 (Millipore) according to the manufacturer's instructions. In particular, FI-T cells were activated with OKT3 and anti-CD28 mAbs in presence of IL-2 (50 U/ml or 2000 U/ml) or IL-7 and IL-15 (10 ng/ml and 5 ng/ml, respectively). T cells were fed twice a week. At days 3, 7 and 10 of culture, supernatants and T cells were collected and 60 μg of sample were tested per well.

***p53* chromatin immunoprecipitation (ChIP) assay.** LTE-T cells, $CD45RA^+$ and $CD45RO^+$ T cells were collected and fixed with formaldehyde (Merck, Darmstadt, Germany) to a final concentration of 1%. Fixation proceeded at room temperature for 10 min and was stopped by the addition of glycine to a final concentration of 0.125 mol/liter. The cells were then washed twice

doi:10.1038/nm.3833

with cold PBS. Pellets were resuspended in 350 µl of lysis buffer and protease inhibitors mixture (Active Motif, Carlsbad, CA), washed and resuspended in 350 µl of optimized ChIP lysis buffer and protease inhibitors mixture (0.5% SDS, 10mM EDTA, 0.5 mM EGTA and 50 mM Tris-HCl, pH 8) and sonicated into chromatin fragments of an average length of 500 bp, as determined empirically by agarose gel electrophoresis of fragmented chromatin samples. Chromatin was kept at −80 °C. The chromatin solution was incubated with a *p53*-specific antibody that recognizes the full-length human protein (no. FL393, Santa Cruz) at 4 °C overnight with rotation. The immunoprecipitation was performed using Chip-IT Express kit (Active Motif, Carlsbad, CA) according to the manufacturer's instructions. Amplifications (37 cycles) were performed using specific primers (**Supplementary Fig. 11**), yielding PCR products ~200 bp in length (location of primers relatively to the origin of the promoter is indicated in parentheses after each primer pair). PCR products were separated by 1.5% agarose electrophoresis in Tris-borate-EDTA buffer and stained with ethidium bromide.

Retroviral constructs, transient transfection and transduction of T lymphocytes. *HPSE* cDNA (accession number NM_006665) was cloned into the SFG retroviral backbone that also encodes the GFP (SFG.HPSE(I)GFP) (**Supplementary Fig. 12**). The construct for the GD2-specific CAR containing the CD28, OX40 and ζ endodomains was previously described (SFG.CAR)[34]. We then generated a bicistronic vector to co-express the *HPSE* and CAR-GD2 using an IRES (SFG.CAR(I)HPSE) (**Supplementary Fig. 12**). The retroviral vector encoding the fusion protein GFP–firefly luciferase (GFP.FFLuc) for *in vivo* imaging of T cells and CD19-specific and CSPG4-specific CARs were previously described[35]. Transient retroviral supernatant was produced as previously described[35]. A specific inhibitor of HPSE, Roneparstat (SST0001) (a chemically modified heparin ^{100}Na,Ro-H, property of Sigma-tau Research Switzerland S.A.) (3 µg ml)[13,36,37], was added to the media during the virus preparation to increase its titer. Activated T lymphocytes were then transduced with retroviral supernatants using retronectin-coated plates (Takara Bio Inc., Shiga, Japan). After removal from the retronectin plates, T cell lines were maintained in complete T cell medium in a humidified atmosphere containing 5% CO_2 at 37 °C in the presence of IL-2 (50 U mL) for 2 weeks.

Flow cytometry. We performed flow cytometry analysis using the following antibodies: antibodies specific to CD45, CD56, CD8, CD4, CD3, CD45RA, CD45RO, CD62L, 7AAD and annexin V (all from Becton Dickinson, San Jose, CA) and CCR7 (from E&D) conjugated with FITC, PE, PerCP or APC fluorochromes. Expression of GD2 and CSPG4 antigens on tumor cell lines was assessed with anti-GD2 (clone 14.g2a, BD) and anti-CSPG4 (clone no. 1E6.4, Miltenyi-Biotec), respectively. The expression of GD2-specific CAR was detected using a specific anti-idiotype antibody (1A7). Samples were analyzed with a BD FACScalibur system equipped with a filter set for quadruple fluorescence signals and the CellQuest software (BD Biosciences). For each sample we analyzed a minimum of 10,000 events.

Chromium-release assay. The cytotoxic activity of T cells was evaluated using a standard 6-h ^{51}Cr-release assay.

Xenogenic mouse models. We used the NSG mouse model to assess the *in vivo* antitumor effect of control and transduced T cells. All mouse experiments were approved by the Institutional Animal Care and Use Committee of Baylor College of Medicine. 8–10-week-old male and female NSG mice (Jackson Laboratory, Bar Harbor, Maine) were injected i.p. with either CHLA-255 or LAN-1 neuroblastoma cells ($GD2^+$) (2.5×10^6) or SENMA melanoma cells ($CSPG4^+$) (5×10^5) resuspended in Matrigel (BD Biosciences). These tumor cell lines were labeled with Firefly luciferase. 10–12 d after neuroblastoma inoculation and 2 d after melanoma inoculation, LTE-T cells were injected i.p. (2×10^7 cells per mouse). No randomization was used. Investigators were not blinded, but mice were matched based on the signal of tumor cells before assignment to control or treatment groups. Mice were euthanized when signs of discomfort were detected by the investigator or as recommended by the veterinarian who monitored the mice three times a week. When valuable, tumor growth was also monitored by bioluminescence. For the *in vivo* biodistribution of T cells, 5×10^6 LTE-T cells per mouse labeled with the GFP.FFluc vector were infused via tail injection. For *in vivo* imaging, we used the Xenogen-IVIS Imaging System as previously described[35]. In the orthotopic model[26], an inoculum of 10^6 CHLA-255 luciferase-transduced tumor cells suspended in 0.1 ml of PBS was surgically implanted under the renal capsule of 5–7-week-old female mice using a 27-gauge needle. CAR^+ and $CAR(I)HPSE^+$ LTE-T cells were infused i.v. ($1–1.5 \times 10^7$ per mouse) 7 d later, and tumor regression was measured by bioluminescence imaging. By day 10, some mice were sacrificed and tumors collected, fixed and stained with anti-human CD3 mAb (no. A0452, Dako North America Inc., Carpinteria, CA). Mice were euthanized when signs of discomfort were detected by the investigator or as recommended by the veterinarian who monitored the mice three times a week or when luciferase signal reached 7.5×10^7 photons per second per cm^2 to investigate animal survival. For the lymphoma model, mice were infused i.v. with Daudi cells (2×10^6 cells) labeled with firefly luciferase. Four days later they were infused i.v. with 10^7 control or CAR^+ and $CAR(I)HPSE^+$ LTE-T cells specific for the CD19 antigen. Tumor growth was measured by bioluminescence imaging. Mice were euthanized when signs of discomfort were detected by the investigator or as recommended by the veterinarian who monitored the mice three times a week.

Tissue processing and immunohistochemistry. Tissue samples were fixed, processed and stained according to standard procedures. We performed H&E staining and labeling of human T cells using polyclonal rabbit anti-human CD3 mAb (A0452, Dako North America Inc., Carpinteria, CA) and for detection we used Dako LSAB + System-HRP (K0679, Dako). Tumors were scored without knowledge of the treatment used by the pathologist (M. Ittmann) by counting human infiltrating T lymphocytes in ten high-power fields at the edge of the tumor.

Statistical analyses. Unless otherwise noted, data are summarized as mean ± s.d. Student's *t*-test (two-sided) was used to determine statistically significant differences between samples, with $P < 0.05$ indicating a significant difference. When multiple comparison analyses were required, statistical significance was evaluated by a repeated-measures ANOVA followed by a log-rank (Mantel–Cox) test for multiple comparisons. The mouse survival data were analyzed using the Kaplan–Meier survival curve, and Fisher's exact test was used to measure statistically significant differences. Animals were excluded only in the event of their death after tumor implant but before T cell infusion. Neither randomization nor blinding was done during the *in vivo* study. However, mice were matched based on the tumor signal for control and treatment groups before infusion of control or gene modified T cells. When bioluminescence signal intensity was used to monitor tumor growth, values were log transformed and then compared using a two-sample *t*-test. In contrast, the analysis of the pathologist M. Ittmann, aimed at quantifying tumor infiltration by human T cells, was performed in a blinded fashion. We estimated the sample size considering the variation and mean of the samples. We tried to reach a conclusion using as small a sample size as possible. We estimated the sample size to detect a difference in means of 2 s.d. at the 0.05 level of significance with 80% power. Graph generation and statistical analyses were performed using Prism version 5.0d software (GraphPad, La Jolla, CA).

31. Yvon, E. *et al.* Immunotherapy of metastatic melanoma using genetically engineered GD2-specific T cells. *Clin. Cancer Res.* **15**, 5852–5860 (2009).
32. Roy, M. *et al.* Antisense-mediated suppression of Heparanase gene inhibits melanoma cell invasion. *Neoplasia* **7**, 253–262 (2005).
33. Zhang, L., Sullivan, P., Suyama, J. & Marchetti, D. Epidermal growth factor-induced heparanase nucleolar localization augments DNA topoisomerase I activity in brain metastatic breast cancer. *Mol. Cancer Res.* **8**, 278–290 (2010).
34. Pulè, M.A. *et al.* A chimeric T cell antigen receptor that augments cytokine release and supports clonal expansion of primary human T cells. *Mol. Ther.* **12**, 933–941 (2005).
35. Vera, J. *et al.* T lymphocytes redirected against the kappa light chain of human immunoglobulin efficiently kill mature B lymphocyte-derived malignant cells. *Blood* **108**, 3890–3897 (2006).
36. Naggi, A. *et al.* Modulation of the heparanase-inhibiting activity of heparin through selective desulfation, graded N-acetylation, and glycol splitting. *J. Biol. Chem.* **280**, 12103–12113 (2005).
37. Zhang, L., Ngo, J.A., Wetzel, M.D. & Marchetti, D. Heparanase mediates a novel mechanism in lapatinib-resistant brain metastatic breast cancer. *Neoplasia* **17**, 101–113 (2015).